

UNIVERSITÀ DEGLI STUDI DI PADOVA

PHYSICS LABORATORY

---

# Timing

---

*Autori:*

Luca MORSELLI  
Andrea RAGGIO

*Docenti:*

Luca STEVANATO  
Francesco RECCHIA

January 20, 2018

## Introduction

In particle detection one of the first and most important requirements is the production of a time reference for detected events. Correct definition of a particle detection time is essential to allow the production of coincidence signals between the different detectors which compose the arrays of an experimental set-up. Moreover the reduction of timing error is crucial for several measurements, such as the *Time of Flight* (TOF) technique, used to distinguish the particle type but also to measure its kinetic energy.

There are several ways to produce a timing reference for detected particles, the aim of a good technique is to increase the accuracy and reduce the dependence on particle energy (*Time walk*). The simplest one is the *Leading Edge* method, which associates the time reference of the signal with the crossing moment of a fixed threshold, for instance 0.2 as shown in Fig. 1-a. In scintillation detectors, where the rising time of the pulses is constant, this method is clearly affected by the amplitude of the signals, making it not good for the purpose. A better solution is the *Constant Fraction Discrimination* (CFD) technique (Fig. 1-b), which gives a time reference independent on pulse amplitude.

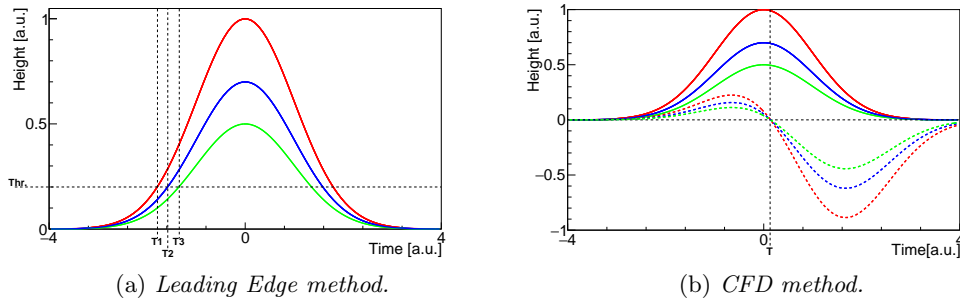


Figure 1: *Leading Edge* (a) and *Constant Fraction Discrimination* (CFD) (b) techniques applied on three Gaussian pulses with same mean and sigma but different amplitudes. The bipolar dashed pulses in b) are generated by the CFD algorithm.

The aim of this report is to present the timing analysis performed over two scintillation detectors. Therefore the following sections will analyze these steps:

- Energy calibration of the organic scintillators and calculation of the energy resolution from the analysis of the Compton edge.
- Optimization of the external delay of the analogue CFTD to obtain the best time resolution.
- Study the time resolution behaviour as a function of the energy.
- Comparison between the timing resolutions obtained from analogue and digital treatment of the signals.
- Measurement of the speed of light.

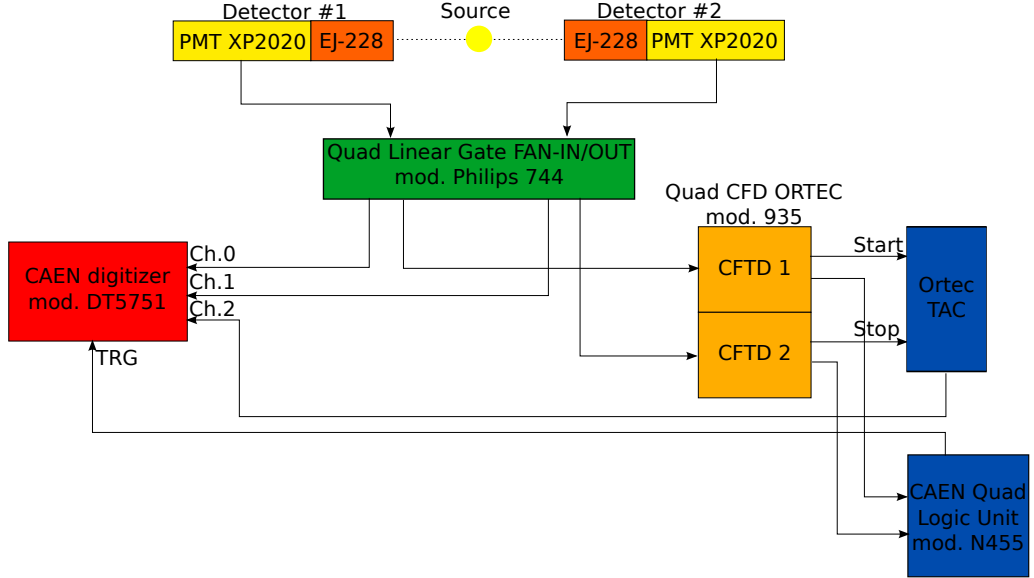


Figure 2: Experimental configuration used in the timing analysis.

## Energy Calibration

In this experiment we have used two cylindrical organic scintillators EJ-228, with a 5 cm diameter and 5 cm thickness. Due to the organic composition of our detectors the photo-electric cross-section of its constituents is negligible for the energy used in laboratory. Furthermore due to the limited size of the detectors total absorption through multiple Compton scattering is negligible too. The detectors response will be dominated by the individual Compton interaction, the result in the energy spectrum is a continuous distribution that corresponds to different angles of interaction. This can be seen in the spectra acquired with the  $^{22}\text{Na}$  source (Fig. 3).

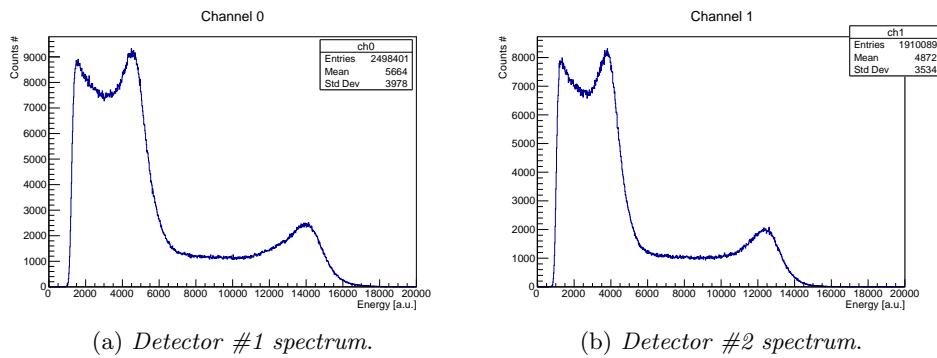


Figure 3: Detectors spectra (not calibrated).

The finite resolution of our detectors result in a shift towards lower energies depending on the detector resolution (Fig. 4).

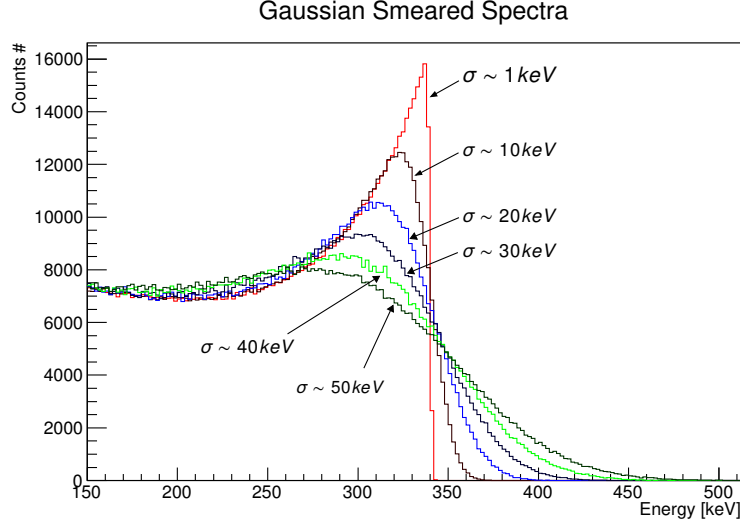


Figure 4: Gaussian smeared spectra at different  $\sigma$  for 511 keV photon.

In order to obtain the energy calibration parameters we have to generate several smeared spectra using the Klein-Nishina cross-section for Compton Scattering:

$$\frac{d\sigma}{dT} = \frac{\pi r_e^2}{m_e c^2 \alpha^2} \left( 2 + \frac{s^2}{\alpha^2 (1-s)^2} + \frac{s}{1-s} \left( s - \frac{2}{\alpha} \right) \right)$$

for 511 keV and 1275 keV respectively. Then we have to subtract the Compton background from acquired spectra in order to search for Compton edge position (Fig. 5).

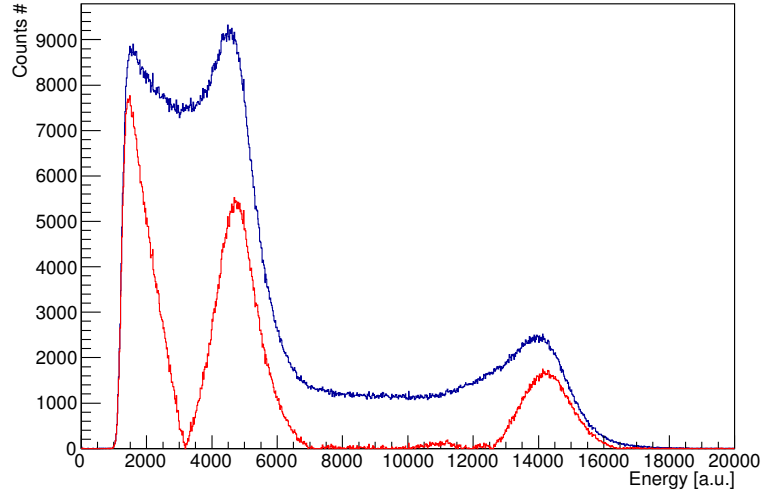


Figure 5: Acquired Spectra (blue). Spectra with subtracted Compton background (red).

Once we have the compton edge position we have to loop on every previous generated smearing and calculating the  $\chi^2$  between experimental spectrum and

gaussian smeared one selecting the smearing with the  $\sigma$  that led to minimum  $\chi^2$ . Once we have selected a proper  $\sigma$  we have also the corresponding shift of the Compton Edge that we have to use in order to calibrate our detector.

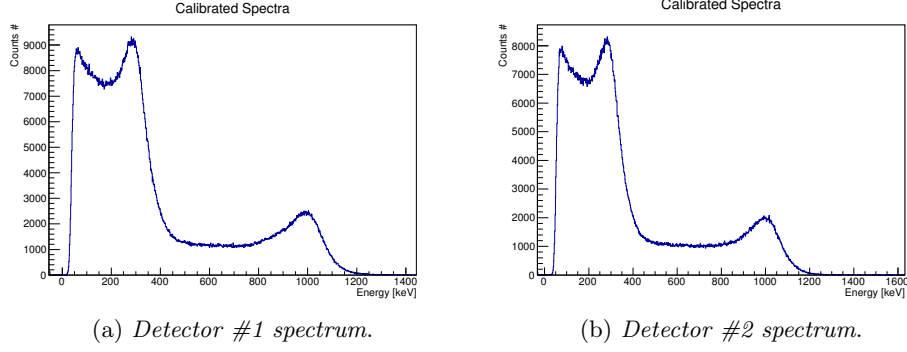


Figure 6: Calibrated detectors spectra.

Photon Energy [keV]	$\sigma$ [keV]	C.E. shifting [keV]
511	34	40.66
1275	40	52.15

Table 1:  $\sigma$  and C.E. shift for detector #1.

Photon Energy [keV]	$\sigma$ [keV]	C.E. shifting [keV]
511	28	34.66
1275	40	52.15

Table 2:  $\sigma$  and C.E. shift for detector #2.

Detector	a [keV/channel]	b [keV]
#1	$0.0748945 \pm$	$-54.2511 \pm$
#2	$0.083215 \pm$	$-32.6856 \pm$

Table 3: Calibration parameters.

## TAC calibration

In order to calibrate the TAC we have acquired data using auto coincidence between a detector signal and itself. By changing the delay in the delay unit we have obtained the spectra in the Fig. 7. Then using TSpectrum we have found the peaks centroid and fit the using a linear function (Fig. 8). The calibrated spectra is shown in Fig. ??.

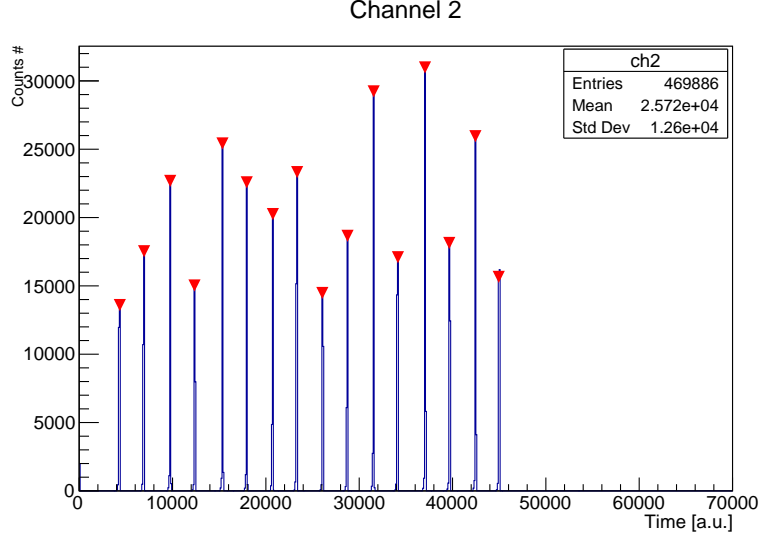


Figure 7: TAC spectrum (not calibrated). Obtained with an autocoincidence.

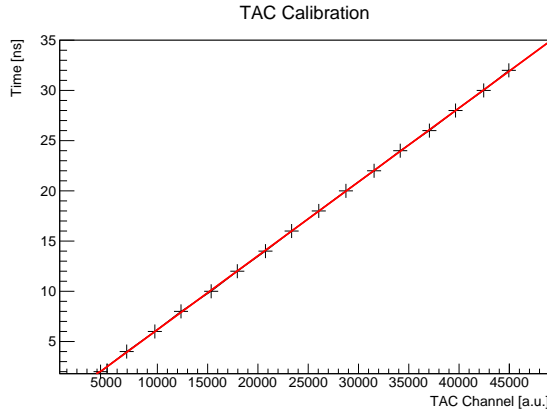


Figure 8: Fit for TAC calibration.

Parameter	Value
p0	$-1.19 \pm 0.04$
p1	$0.000736 \pm 0.000001$

Fit parameters.

## External delay optimization

### Time resolution behaviour as a function of energy

In order to study the time resolution dependence as a function of the energy we have used a different radioactive source,  $^{60}\text{Co}$ . This source is chosen because of its high energy Compton Edge (1 MeV) that allow us to study the energy dependence up to this energy.

By imposing a lower energy threshold starting from 100 keV to 1000 keV we are able to plot the time resolution as a function of the lower energy threshold (Fig.11 ).

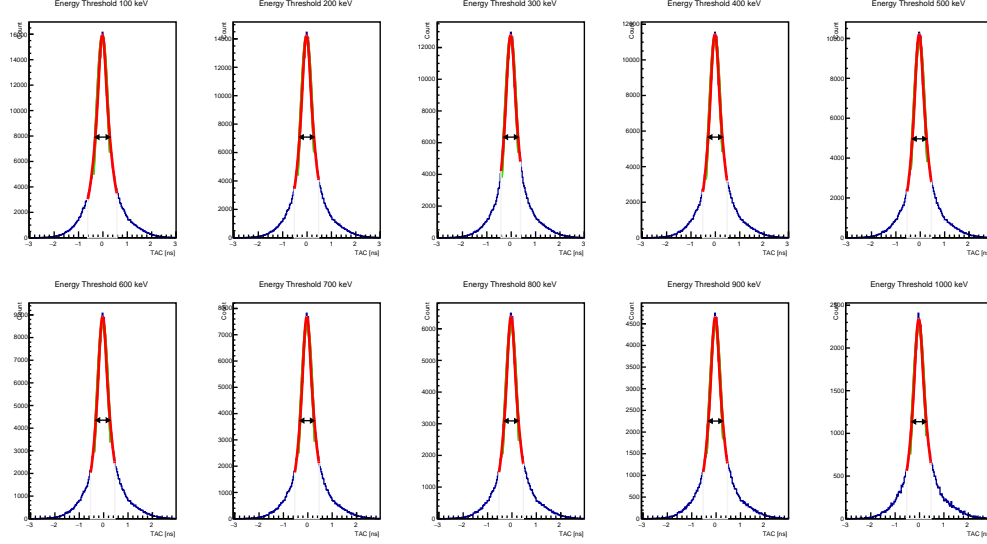


Figure 9: Timing distributions using threshold.

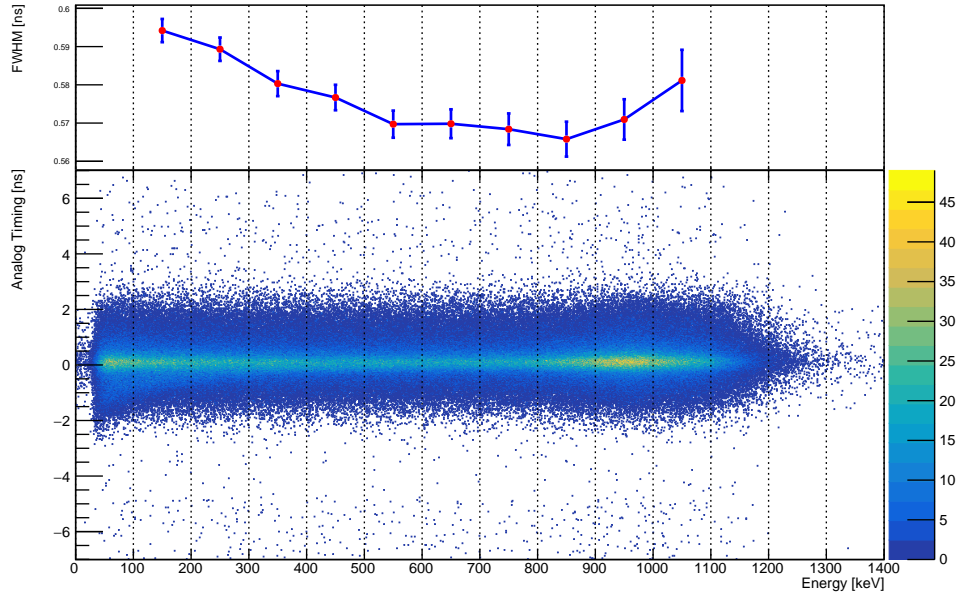


Figure 10: Lower energy threshold.

We can also proceed in a slightly different way: instead of setting a lower energy threshold we can select energy windows with 100 keV of width and plotting the time resolution in function of the energy mid-energy (Fig. 12 ).

The time resolution behaviour obtained with these two different methods have the same shape but we can clearly see that the use of energy windows allow to determine the time resolution with a lower constant error due to the fact that we

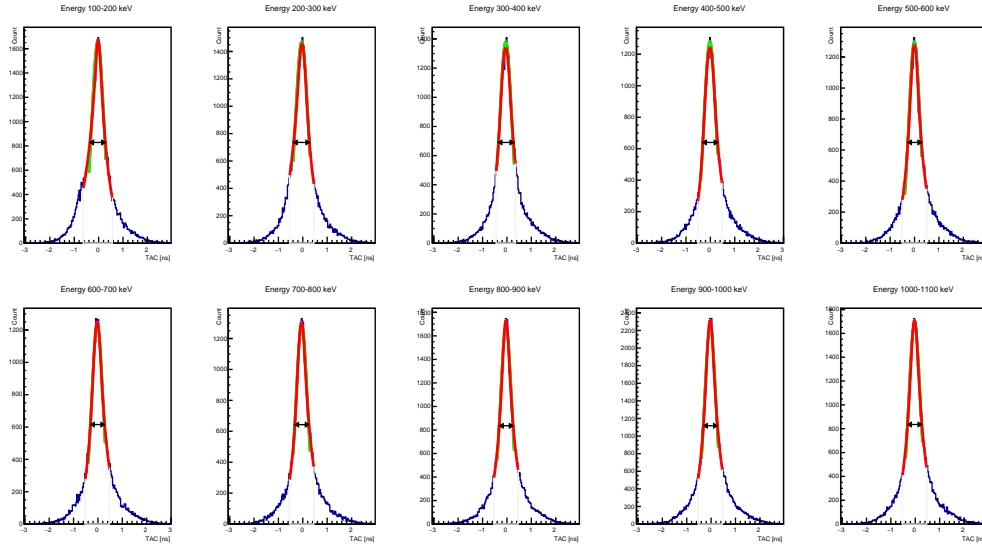


Figure 11: Timing distributions using threshold.

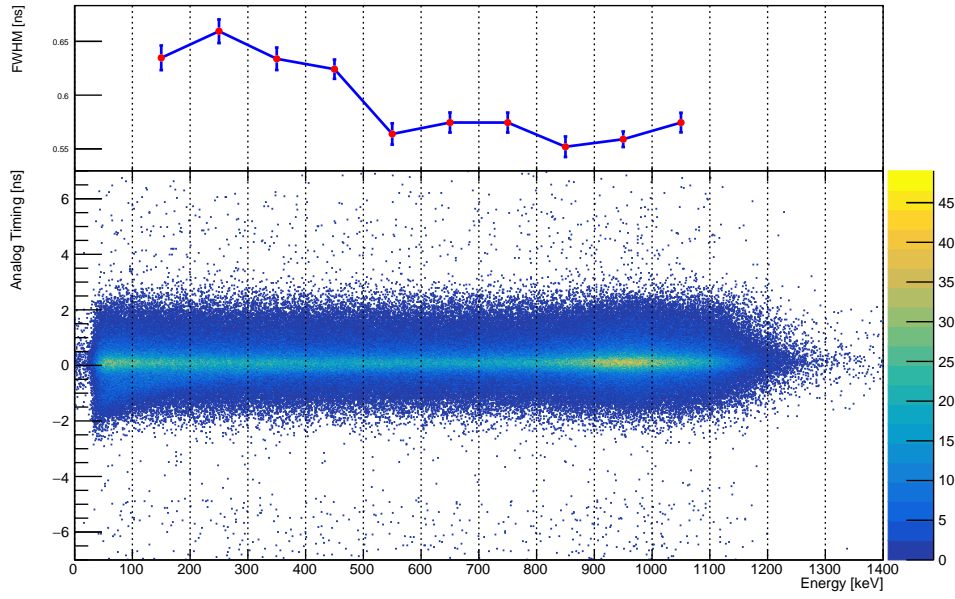


Figure 12: Energy Windows

## Digital Timing

We can perform a digital timing that reconstructs all the analog chain using software. In order to do so we need the signal waveforms provided by the DT5751 CAEN digitizer<sup>1</sup>. The digitized waveform then is manipulated in order to obtain a bipolar signal (Fig.13). Then thought out an algorithms we have to find the zero of the signal that is the time that we associate to the event.

descrizione dell'algoritmo e del fit c2 etc etc

The bipolar signal shape depends on two parameter that we need to tune in order

<sup>1</sup>with a sampling rate of 1 GS/s



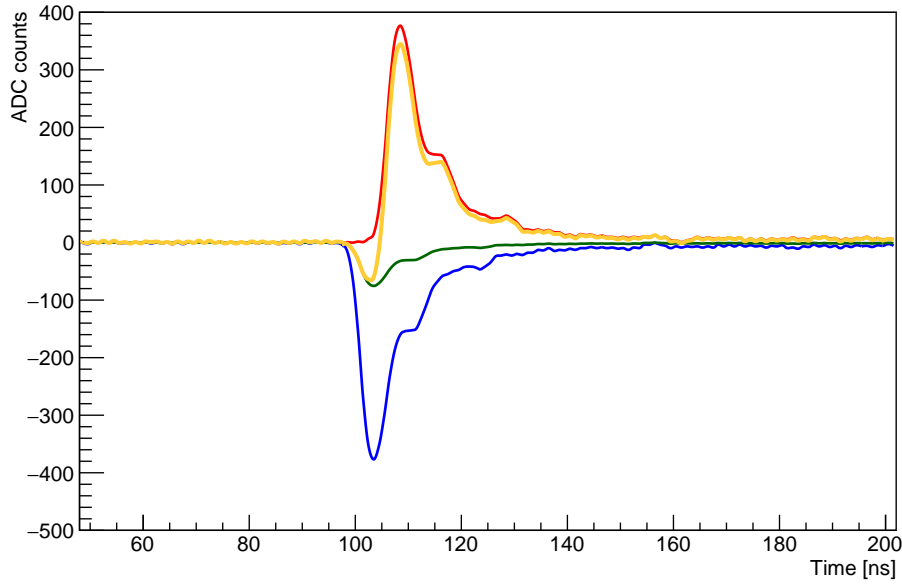


Figure 13: Digital waveforms manipulations used to get the bipolar signal

to optimize the time resolution:

- Fraction
- Delay

## Speed of light

Lorem ipsum dolor sit amet, consectetur adipiscing elit. Ut purus elit, vestibulum ut, placerat ac, adipiscing vitae, felis. Curabitur dictum gravida mauris. Nam arcu libero, nonummy eget, consectetur id, vulputate a, magna. Donec vehicula augue eu neque. Pellentesque habitant morbi tristique senectus et netus et malesuada fames ac turpis egestas. Mauris ut leo. Cras viverra metus rhoncus sem. Nulla et lectus vestibulum urna fringilla ultrices. Phasellus eu tellus sit amet tortor gravida placerat. Integer sapien est, iaculis in, pretium quis, viverra ac, nunc. Praesent eget sem vel leo ultrices bibendum. Aenean faucibus. Morbi dolor nulla, malesuada eu, pulvinar at, mollis ac, nulla. Curabitur auctor semper nulla. Donec varius orci eget risus. Duis nibh mi, congue eu, accumsan eleifend, sagittis quis, diam. Duis eget orci sit amet orci dignissim rutrum.

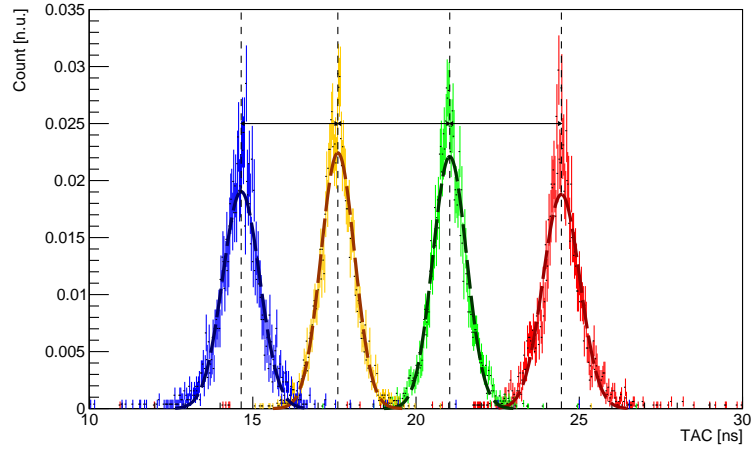


Figure 14: TAC distribution in the four different positions.

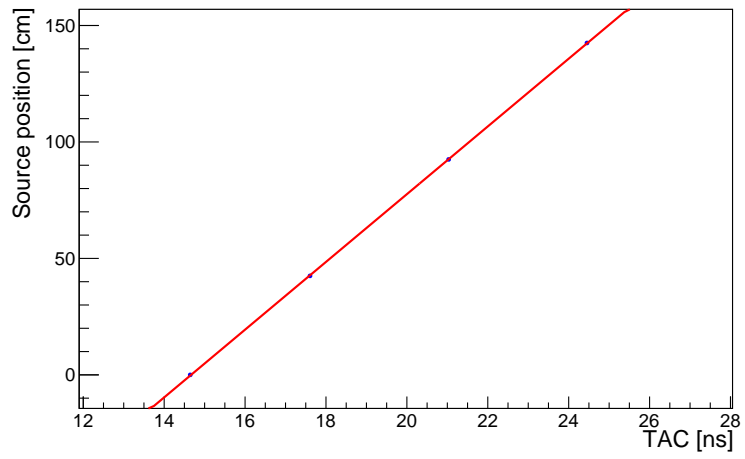


Figure 15: Position vs Time (the angular coefficient is  $c/2$ ).